0013-7227/99/$03.00/0
Endocrinology
Copyright © 1999 by The Endocrine Society
Vol. 140, No. 12
Printed in U.S.A.

Ceramide Inhibits L-Type Calcium Channel Currents in Rat Pinealocytes*

C. L. CHIK, B. LI, T. NEGISHI, E. KARPINSKI, AND A. K. HO

Departments of Physiology and Medicine (C.L.C.), Faculty of Medicine, University of Alberta, Edmonton, Alberta, Canada T6G 2H7

ABSTRACT

In rat pinealocytes, ceramide can inhibit the KCl- and BayK 8644-mediated potentiation of cAMP and cGMP accumulation, suggesting that the L-type Ca^{2+} channel is a target of ceramide action. This was examined in the present study using intracellular Ca^{2+} measurement and patch-clamp studies. In fura-2-loaded pinealocytes, C2- and C6-ceramide inhibited the Ca^{2+} increase caused by BayK 8644 and KCl, but not that caused by norepinephrine, suggesting an inhibitory effect of ceramide on the L-type Ca^{2+} channels. Patch-clamp analysis confirmed that C2- and C6-ceramide, but not C2-dihydroceramide (the inactive analog) inhibited the L-type Ca^{2+} channel current. Furthermore, treatments known to increase cellular ceramide levels, including a glucosylceramide synthase inhibitor and sphingomyelinase, also inhibited this current. The inhibitory effect of ceramide on the current was attenuated by lavendustin A, a tyrosine kinase inhibitor, but not by H7, a serine/threonine kinase inhibitor. The effect of ceramide was mimicked by interleukin-1β, a cytokine highly expressed in the pineal that is known to activate the sphingomyelin pathway. These results indicate that the sphingomyelin pathway is another important signaling mechanism that regulates the L-type Ca^{2+} channel, and tyrosine kinase appears to be involved in the effect of ceramide. (*Endocrinology* **140:** 5682–5690, 1999)

L-TYPE Ca^{2+} channels (L-channels) play an important role in the control of pineal function, including melatonin synthesis (1, 2). Using the whole cell version of the patch-clamp technique, we have shown that rat pinealocytes express the L-type, but not the T- or N-type, Ca^{2+} channel (3, 4). These channels are activated by the nicotinic subtype of cholinergic receptors (1, 2). They are also regulated by adrenergically mediated mechanisms through cAMP- and cGMP-dependent protein kinases (3, 4). Growth factors, including insulin-like growth factor I and insulin, have also been shown to modulate these channels through a tyrosine kinase-dependent mechanism (5).

Another signaling mechanism that could modulate Ca^{2+} channel activity is the sphingomyelin pathway (6). This pathway mediates the action of cytokines such as interleukin-1β, interferon-γ, and tumor necrosis factor-α (7–9). Ceramide is produced after sphingomyelin hydrolysis by activation of a sphingomyelinase (9). The ceramide generated can function as a second messenger (9). Direct targets of ceramide that have been identified include specific kinases and phosphatases that are coupled to signaling mechanisms, including mitogen-activated protein kinases and phospholipase D (10–14). The importance of kinases and phosphatases in the modulation of L-channels in rat pinealocytes (3–5, 15) suggests that L-channels are probably regulated by ceramide in rat pinealocytes. This was also supported by our recent observation that ceramide selectively inhibits the KCl- and BayK 8644-mediated potentiation of β-adrenergically stimulated cAMP and cGMP accumulation (16). In this study, we investigated whether ceramide had an acute effect on the pineal L-channels using intracellular Ca^{2+} measurement and patch-clamp analysis. We found that ceramide inhibits the L-channels in rat pinealocytes and that this inhibition is mediated in part by tyrosine kinases.

Materials and Methods

Materials

Sphingomyelinase was obtained from Sigma Chemical Co. (St. Louis, MO). BayK 8644, C2- and C6-ceramide, C2-dihydroceramide, H89, human recombinant interleukin-1β, KT5823, lavendustin A, lavendustin B, and 1-phenyl-2-hexadecanoylamino-3-morpholino-1-propanol (PPMP) were obtained from Calbiochem (La Jolla, CA). Fura-2/AM was obtained from Molecular Probes, Inc. (Eugene, OR). Cs_2-aspartate was prepared by Dr. H. J. Liu (Department of Chemistry, University of Alberta, Edmonton, Canada). [^{125}I]cAMP and [^{125}I]cGMP were obtained from ICN Immunobiologicals (Lisle, IL). All other chemicals were of the purest grade available and were obtained commercially. Antibodies for the RIAs of cAMP and cGMP were gifts from Dr. A. Baukal (NICHHD, NIH, Bethesda, MD).

Cell preparations

All procedures were reviewed and approved by the health sciences animal and welfare committee of the University of Alberta. Male Sprague Dawley rats (150 g) were decapitated after cervical dislocation. Pinealocytes were then prepared by trypsinization as described previously (17). The cells were suspended in DMEM containing 10% FCS and were maintained overnight at 37 C in a mixture of 95% air and 5% CO_2.

Ca^{2+} channel current recordings were obtained using the whole cell version of the patch-clamp technique (18). Patch electrodes were pulled from borosilicate glass capillary tubes (od, 1.2 mm; id, 0.9 mm; FHC, Brunswick, ME) and heat polished. They were filled with a solution containing 70 mM Cs_2-aspartate, 20 mM HEPES, 11 mM EGTA, 1 mM $CaCl_2$, 5 mM $MgCl_2$·$6H_2O$, 5 mM glucose, 5 mM ATP-Na_2, and 5 mM K-succinate. Creatine phosphokinase (50 U/ml) and phosphocreatine-Na_2 (20 mM) were added to the pipette solution to reduce current run down. The bath solution contained 105 mM Tris-Cl, 0.8 mM $MgCl_2$·$6H_2O$, 5.4 mM KCl, 20 mM $BaCl_2$, 0.02 mM tetrodotoxin, and 10 mM HEPES. Ba^{2+} (20 mM) was used as the charge carrier. All solutions were filtered (0.22 μm) before use. The osmolarity was adjusted to 320 mosmol, and the pH

Received June 2, 1999.

Address all correspondence and requests for reprints to: Dr. C. L. Chik, Department of Medicine, 7–33 Medical Sciences Building, Edmonton, Alberta, Canada T6G 2H7. E-mail: cchik@ualberta.ca.

* This work was supported by grants from the Medical Research Council of Canada.

Downloaded from https://academic.oup.com/endo/article/140/12/5682/2990682 by guest on 20 August 2022

was adjusted to 7.4. The membrane currents were measured using an Axopatch 1B whole cell patch-clamp amplifier (Axon Instruments, Foster City, CA). The data were filtered at 5 kHz and sampled at 10 kHz using pClamp software (pClamp 7) and a Digidata 1200B analog to digital interface (Axon Instruments, Foster City, CA). Analysis was performed using the pClamp software. To generate current-voltage (I-V) relationships, 250-msec depolarizing test pulses of increasing amplitude were applied at a frequency of 0.3 Hz. On-line leakage subtraction was implemented using the P/2 protocol in pClamp software. At a holding potential of −50 mV and with Cs^+ in the internal solution, hyperpolarizing pulses did not activate any currents, and identical results were obtained with the P/2 or P/4 protocol. The experiments were performed at room temperature (20–22 C).

Pineal cells were evaluated for current run down before they were used for experiments. After the whole cell configuration was established, the current amplitude increased for 2–3 min due to inhibition of the outward K^+ current by intracellular Cs^+. When the current reached its peak amplitude, it was monitored for an additional 5 min to estimate the run down rate. In 90% of cells, the initial run down rate was less than 5%, and a stable current could be recorded for the next 30 min. In 10% of cells, the initial run down rate was more than 5%. These cells tended to continue to run down and were not used for experiments. If the initial run down rate was less than 5%, the drugs were added to the bath solution after 5 min.

The steady state inactivation and activation as described by the normalized conductance was obtained from deactivation tail current amplitude, normalized, and fitted to a Boltzman function of the form $G = G_{max}(1/1 + \exp(V_{1/2} - V_x)/k)$, where G is the normalized conductance, G_{max} is the maximal conductance, $V_{1/2}$ is the voltage at which half of the macroscopic current is activated, V_x is the test voltage, and k is the slope. The magnitude of the tail currents was obtained by fitting the data to two exponential components. The fitting of exponentials to whole cell tail currents was performed using Clampfit (version 6.05). A simplex algorithm was used to find the sum of least square error fits. Iterative fits converged when the simplex fractional error became less than 0.0001. In all fits, the first 250 μsec were ignored to avoid artifacts produced by the settling of the voltage clamp. The amplitude values that were used to construct the normalized conductance curves were extrapolated to the time of repolarization. The tail currents for activation curves were activated from a holding potential of −50 mV to various test potentials and repolarized to −50 mV. To obtain the steady state inactivation, the holding potential was varied from −90 to +25 mV. The test pulse was +50 mV, with repolarization to −50 mV.

Data are presented as the mean ± SEM percentage of control values. At least three different cell preparations were used for each study. The pretreatment I-V relationship was plotted and used as a control. The effects of the drugs were monitored continuously using depolarizing pulses at a frequency of 0.03 Hz, except when generating I-V relationships. Paired *t* test was used for comparison between control values and those obtained after drug administration. All histograms were corrected for average current rundown at 15 min, which was 5.7 ± 0.4% (n = 6). In the case of multiple comparisons, ANOVA in conjunction with the Newman-Keuls test was applied.

cAMP and cGMP assays

cAMP and cGMP measurements were made on samples of cells (15,000 cells/400 μl) treated with various agents for 15 min; the RIA method of measurement has been described in detail previously (19, 20).

Determination of intracellular Ca^{2+} $[Ca^{2+}]_i$

$[Ca^{2+}]_i$ was determined using a fluorescent Ca^{2+} indicator, fura-2 (21, 22). Briefly, 5×10^5 cells were pelleted and resuspended in culture medium (DMEM with 25 mM HEPES, pH 7.4). The cells were loaded with fura-2 by incubation with fura-2 (5 μM) for 45 min at 37 C. After washing twice with DMEM, the pinealocytes were suspended in a fresh buffered salt solution (buffer B; 140 mM NaCl, 5 mM KCl, 2 mM $CaCl_2$, 1.2 mM $MgCl_2$, 1.2 mM KH_2PO_4, 25 mM HEPES, and 6 mM glucose, pH 7.4). Fura-2-loaded cells (3×10^5 cells/1.5 ml) were transferred to a cuvette for fluorescence signal determination, using an SLM Aminco DMX-1000 fluorescence spectrophotometer (SLM Instruments, Inc., Urbana, IL) with a thermostatically controlled cell holder fitted with a magnetic stirrer. The excitation wavelengths used were 340 and 380 nm, and emission was monitored at 510 nm. Paired *t* test was used for analysis of $[Ca^{2+}]_i$ measurements. Statistical significance was set at 0.05.

Results

C6-ceramide inhibits KCl and BayK 8644 potentiation of isoproterenol-stimulated cyclic nucleotide accumulation

Treatment of pinealocytes with isoproterenol (1 μM) caused a significant increase in cAMP and cGMP accumulation; the addition of depolarizing concentrations of K^+ potentiated the isoproterenol-stimulated cAMP and cGMP accumulation in a concentration-dependent manner as reported previously (16, 23) (Fig. 1). C6-ceramide (30 μM) had no effect on basal cAMP and cGMP accumulation (Table 1). However, C6-ceramide caused an increase in the EC_{50} value of the potentiation by KCl without affecting the maximal

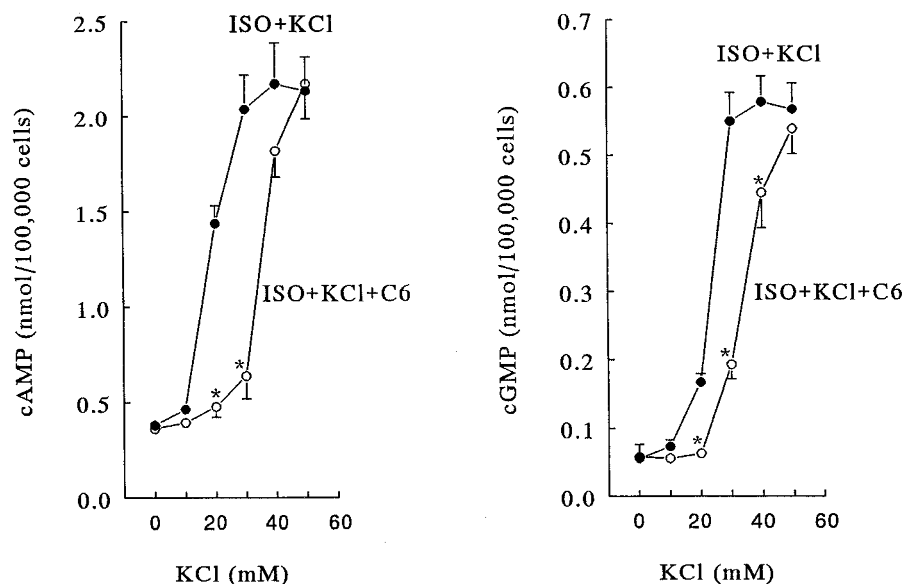

FIG. 1. Effect of C6-ceramide on isoproterenol (ISO)- and KCl-stimulated cAMP and cGMP accumulation in rat pinealocytes. Pinealocytes (1.5×10^4 cells/400 μl) were incubated in DMEM with 10% FBS in the absence or presence of C6-ceramide (C6; 30 μM) for 5 min. The cells were then stimulated with ISO (1 μM) in the presence of varying concentrations of KCl (10–50 mM) for an additional 15 min, and cellular cAMP and cGMP contents were determined. Each value represents the mean ± SEM of determinations performed in quadruplicate from three independent experiments. For further details, see *Materials and Methods*. *, $P < 0.05$ compared with the corresponding treatment without ceramide.

Downloaded from https://academic.oup.com/endo/article/140/12/5682/2990682 by guest on 20 August 2022

TABLE 1. Effects of ceramides on the potentiating effect of K^+ and BayK 8644 on ISO-stimulated cAMP and cGMP responses

Treatment	nmol/10^5 cells	
	cAMP	cGMP
Control	0.05 ± 0.01	0.008 ± 0.002
C6-ceramide (30 μM)	0.06 ± 0.01	0.009 ± 0.001
ISO (1 μM)	0.34 ± 0.04	0.041 ± 0.008
+C6-ceramide (30 μM)	0.39 ± 0.05	0.045 ± 0.001
ISO (1 μM) + KCl (30 mM)	2.35 ± 0.22	0.511 ± 0.011
+C6-ceramide (30 μM)	1.15 ± 0.09[a]	0.205 ± 0.024[a]
+C2-ceramide (30 μM)	1.43 ± 0.12[a]	0.312 ± 0.029[a]
+C2-dihydroceramide (30 μM)	2.15 ± 0.17	0.477 ± 0.031
ISO (1 μM) + BayK 8644 (1 μM)	1.96 ± 0.21	0.445 ± 0.010
+C6-ceramide (30 μM)	0.74 ± 0.04[a]	0.164 ± 0.025[a]
+C2-ceramide (30 μM)	1.11 ± 0.17[a]	0.215 ± 0.027[a]
+C2-dihydroceramide (30 μM)	2.01 ± 0.15	0.442 ± 0.035

Pinealocytes (1.5×10^4 cells/400 μl) were incubated in DMEM with 10% FBS and pretreated with or without ceramides (30 μM) for 5 min. The cells were then stimulated by ISO (1 μM) and KCl (30 mM) or ISO (1 μM) and BayK 8644 (1 μM) for an additional 15 min. Each value represents the mean ± SEM of determinations performed in quadruplicate from three independent experiments.

[a] Significant inhibition by ceramides, $P < 0.05$.

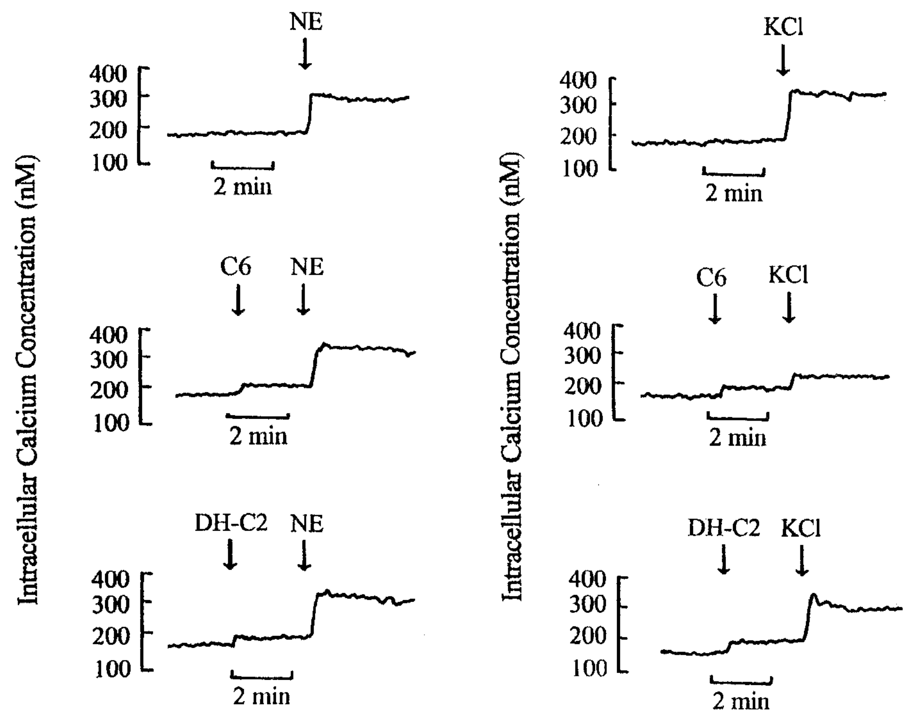

FIG. 2. Effects of ceramides on KCl- and norepinephrine-mediated increases in intracellular Ca^{2+} in rat pinealocytes. Rat pinealocytes were prepared and loaded with the fluorescent Ca^{2+} indicator fura-2. The ratio of the fluorescence emission signal at 510 nm, excited at 340 and 380 nm, was continuously recorded and calibrated as described. The traces are representative of at least three experiments. a, Addition of norepinephrine (NE; 1 μM) alone; b, addition of C6-ceramide (C6; 30 μM) followed by NE (1 μM); c, addition of C2-dihycroceramide (DH-C2; 30 μM) followed by NE (1 μM); d) addition of KCl (30 mM) alone; e) addition of C6 (30 μM) followed by KCl (30 mM); and f) addition of DH-C2 (30 μM) followed by KCl (30 mM). C6-ceramide decreased the KCl-stimulated, but not the NE-stimulated, increases in intracellular Ca^{2+}. For further details, see *Materials and Methods*.

potentiation (Fig. 1). Similar to our previous study (16), C2-ceramide (30 μM) also inhibited the KCl- and BayK 8644-potentiation of isoproterenol-stimulated cyclic nucleotide accumulation (Table 1). In contrast, C2-dihydroceramide (30 μM), the inactive analog, was ineffective (Table 1). These results suggest that the L-channel may be a target of ceramide action.

Ceramide reduces KCl- and BayK 8644-induced increases in $[Ca^{2+}]_i$, but not that induced by norepinephrine

In fura-2-loaded pinealocytes, a depolarizing concentration of K^+ (30 mM KCl) or BayK 8644 (1 μM) caused an increase in $[Ca^{2+}]_i$, as in previous studies (21) (Fig. 2 and Table 2). C6-ceramide, C2-ceramide, or C2-dihydroceramide (30 μM) caused a small increase in the fluorescent signal (Fig. 2 and Table 2), which was caused by autofluorescence, as similar increases were observed in a cell-free system. Treatment with C6- or C2-ceramide was effective in reducing the increase in $[Ca^{2+}]_i$ caused by BayK 8644 or a depolarizing concentration of K^+, whereas C2-dihydroceramide was ineffective (Fig. 2 and Table 2). In contrast, neither C6- nor C2-ceramide had an effect on the increase in $[Ca^{2+}]_i$ caused by norepinephrine (1 μM; Fig. 2 and Table 2).

Treatment with a glucosylceramide synthase inhibitor, PPMP, has been shown to increase cellular ceramide levels (24, 25). PPMP (10 μM), like C6- and C2-ceramide, was effective in reducing the increase in $[Ca^{2+}]_i$ caused by BayK 8644 or by a depolarizing concentration of K^+. However, PPMP (10 μM) had no effect on the increase in $[Ca^{2+}]_i$ caused by norepinephrine (Table 2).

Downloaded from https://academic.oup.com/endo/article/140/12/5682/2990682 by guest on 20 August 2022

TABLE 2. Effect of ceramides and PPMP on KCl-, BayK 8644-, and norepinephrine-mediated increases in intracellular Ca^{2+}

Treatment	Intracellular Ca^{2+} (nM)				
	DMSO	+C2	+C6	+DH-C2	+PPMP
Control	175 ± 3.5	195 ± 4.5	193 ± 5.5	198 ± 4.3	178 ± 4.0
KCl (30 mM)	320 ± 8.5	215 ± 5.4[a]	209 ± 4.5[a]	310 ± 7.5	198 ± 3.5[a]
BayK 8644 (1 μM)	305 ± 6.5	220 ± 4.7[a]	215 ± 4.9[a]	305 ± 6.9	195 ± 4.4[a]
NE (1 μM)	295 ± 9.9	305 ± 7.5	315 ± 9.5	307 ± 8.8	301 ± 4.5

Values are recorded 1 min after drug treatment during the plateau phase and are reported as the mean ± SEM of at least four determinations from three different cell preparations. Rat pinealocytes were prepared and loaded with the fluorescent Ca^{2+} indicator, fura-2. Cells were treated with C2-ceramide (C2; 30 μM), C6-ceramide (C6; 30 μM), C2-dihydroceramide (DH-C2; 30 μM) or PPMP (10 μM) for 2 min before the addition of KCl, BayK 8644, or norepinephrine (NE; 1 μM). For measurement of intracellular Ca^{2+}, see *Materials and Methods*.

[a] Significant inhibition by ceramides or PPMP, $P < 0.05$.

Downloaded from https://academic.oup.com/endo/article/140/12/5682/2990682 by guest on 20 August 2022

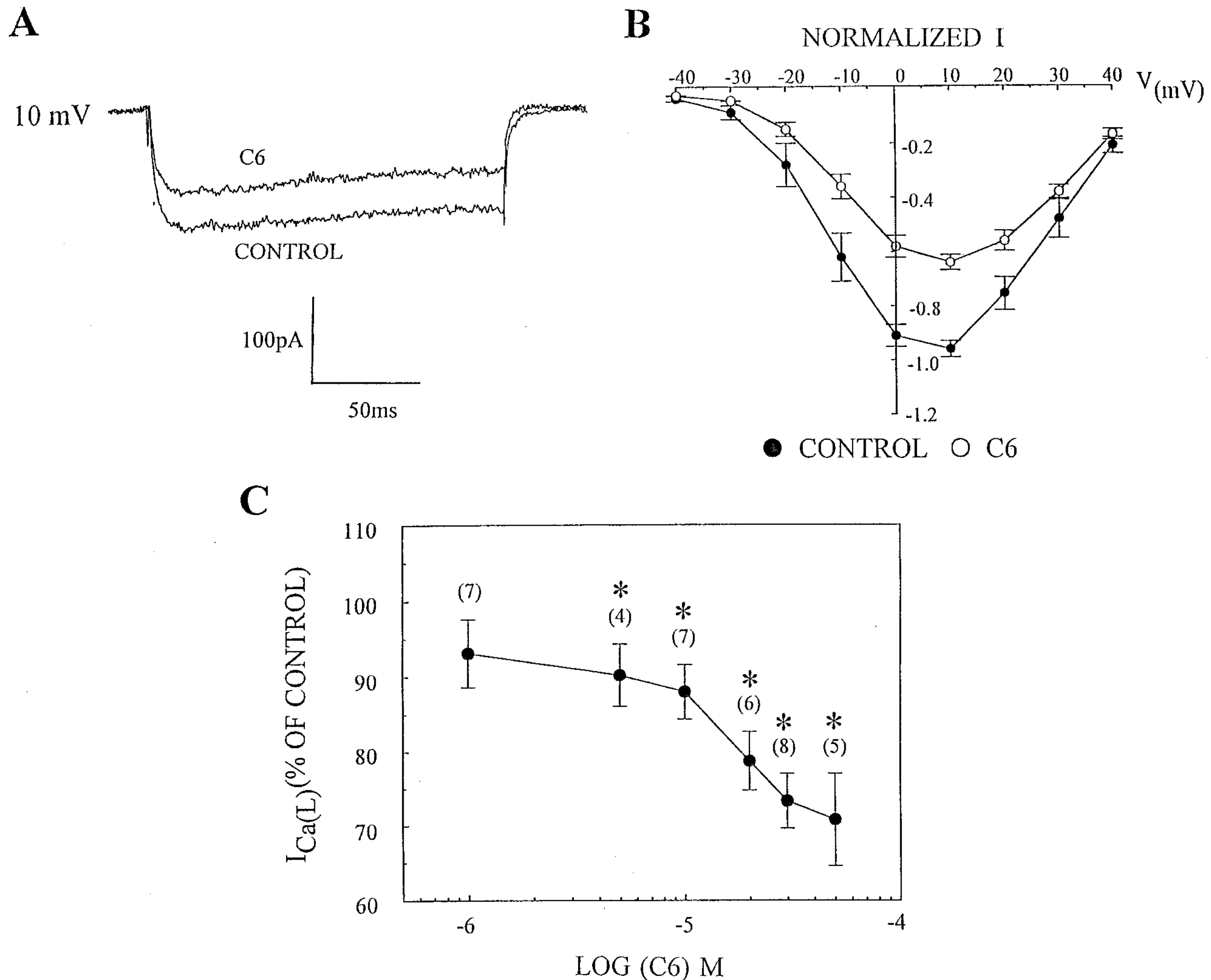

FIG. 3. Effect of C6-ceramide on the L-channel current in rat pinealocytes. A, The L-channel current activated by depolarizing the pinealocyte from −50 to 10 mV in the absence (●) or presence (○) of C6-ceramide (C6; 30 μM). B, The combined I-V relationship from a group of cells in the absence (●) or presence (○) of C6 (30 μM; n = 8). The data were normalized to the peak inward control current. C, The effect of C6 on the L-channel current as a function of concentration. The inhibition 15 min after the addition of C6 was used to obtain the *data points*. The n values are shown in *parentheses above the data points*. *, $P < 0.05$ compared with the control current.

Ceramide inhibits the L-type Ca^{2+} channel current in rat pinealocytes

As reported previously, the only voltage-dependent Ca^{2+} channel current found in dissociated pinealocytes is the dihydropyridine-sensitive L-channel current (3–5). The effect of C6-ceramide on the L-channel current is shown in Fig. 3. The current was activated by depolarizing the cell from −50 to 10 mV before and after C6-ceramide (30 μM; Fig. 3A). C6-ceramide (30 μM) decreased the peak amplitude of the L-channel current by about 30% (Fig. 3A). The data from eight cells were normalized to the peak inward current and plotted as the I-V relationship, as shown in Fig. 3B. Inhibition

of the L-channel current by C6-ceramide was dependent on concentration, with an estimated EC_{50} value of 14 μM; a small inhibition was observed at 5 μM, and the maximal inhibition observed was about 30% at a concentration of 50 μM (Fig. 3C).

The effect of C6-ceramide (30 μM) on the L-channel current as a function of time is shown in Fig. 4A. The onset of the inhibition caused by C6-ceramide occurred within 7–10 min, and maximal inhibition was observed between 12–15 min. The effect of C6-ceramide was not reversed by wash out (data not shown). The current run down from a group of control cells is included for comparison (Fig. 4A). The average current run down at 15 min was 5.7 ± 0.4% (n = 6; Fig. 4A). Although less effective than C6 ceramide, C2-ceramide (30 μM) also inhibited the L-channel current (Fig. 4A). The inhibition by C2- and C6-ceramide persisted in the presence of BayK 8644 (Fig. 4B). In contrast, C2-dihydroceramide (30 μM), an inactive analog, had no effect on basal or BayK 8644-stimulated L-channel current (Fig. 4B).

Further characterization of the effect of C6-ceramide on the L-channel current was carried out by measuring its effect on deactivation tail currents. The deactivation tail currents before and after C6-ceramide (30 μM) treatment are shown in Fig. 5A. The *solid lines* are the exponential fits to the data. C6-ceramide decreased both the amplitude of the peak cur-

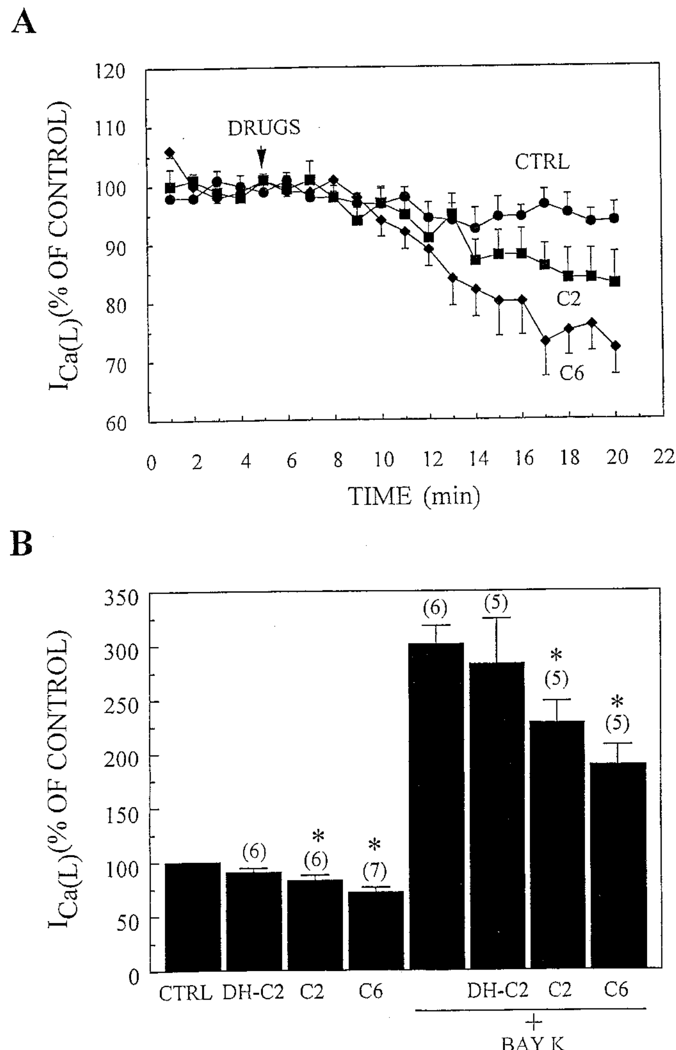

FIG. 4. Effect of ceramides on basal and BayK 8644-activated L-channel current in rat pinealocytes. A, The effect of C2-ceramide (C2; 30 μM) and C6-ceramide (C6; 30 μM) on the L-channel current as a function of time. The peak L-channel current at 1-min intervals was normalized to the current 5 min after the whole cell configuration was established and plotted as a percentage of the control current. Ceramides were applied as shown, and the maximal effect was observed 15 min later. Also shown for comparison is the L-channel current rundown (CTRL). B, The combined data 15 min after the addition of C6 (30 μM), C2 (30 μM), or C2-dihydroceramide (DH-C2; 30 μM). Also shown in B is the decrease in L-channel current caused by ceramides in cells pretreated with BayK 8644 (1 μM) for 5 min. The n values are shown in *parentheses above the data point*. *, $P < 0.05$ compared with the corresponding treatment without ceramide.

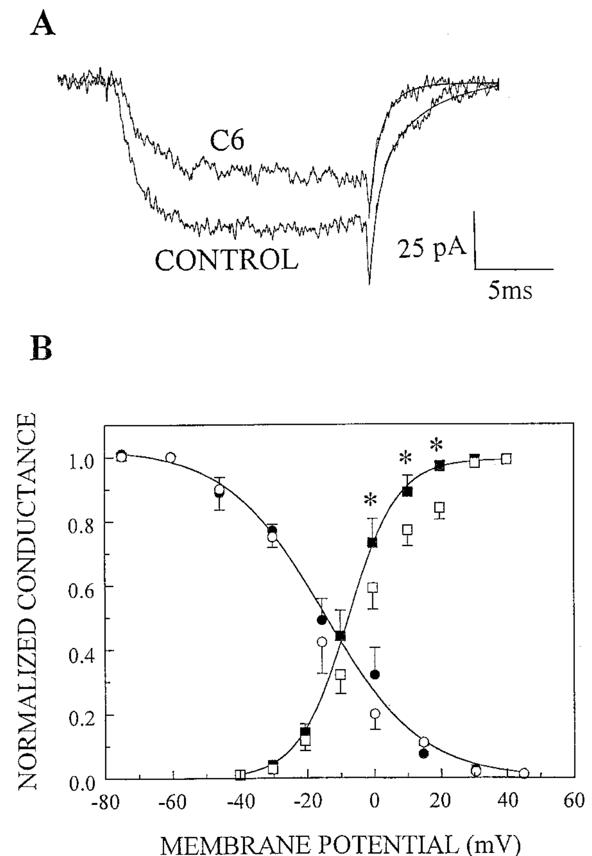

FIG. 5. Effect of C6-ceramide on L-channel steady state activation and inactivation. A, The deactivation tail currents before and after C6-ceramide (C6; 30 μM) were obtained by depolarizing the cell from −50 to 10 mV and then repolarizing to −50 mV. The *solid lines* are the curve fits extrapolated to the time of repolarization. C6 decreased the magnitude of the inward current and the deactivation current tail. B, Using the peak extrapolated amplitude of the deactivation tails, normalized steady state inactivation and activation functions were constructed. The control *data points* (● and ■) were fitted to a Boltzman function (*solid lines*) of the type $G = G_{max}(1/1 + \exp(V_{1/2} - V_x)k)$, where G is the normalized conductance, G_{max} is the maximal conductance, $V_{1/2}$ is the voltage at which half of the macroscopic current is activated, V_x is the test voltage, and k is the slope ($V_{1/2} = -18.0$ mV; k = −8.0 for the inactivation curve and $V_{1/2} = -8.0$ mV; k = 7.5 for the activation curve; n = 6). The *data points* after C6 are shown as ○ and □. C6 had no significant effect on the steady state inactivation. However, C6 shifted the steady state activation toward more positive potentials, with significant differences at 0, 10, and 20 mV (*, $P < 0.05$).

Downloaded from https://academic.oup.com/endo/article/140/12/5682/2990682 by guest on 20 August 2022

rent and the deactivation tail current (Fig. 5A). In Fig. 5B, steady state inactivation and activation as described by normalized conductance are shown. C6-ceramide (30 μM) had no effect on the steady state inactivation, but shifted the activation curve toward more positive membrane potentials. The data points after C6-ceramide at 0, 10, and 20 mV are significantly different from those before treatment with C6-ceramide ($P < 0.05$; Fig. 5B).

Effects of PPMP and sphingomyelinase on the L-channel current

Cellular ceramide levels can be increased by treatment with PPMP, a glucosylceramide synthase inhibitor, which prevents the breakdown of ceramide (24, 25), or sphingomyelinase, which causes membrane hydrolysis of sphingomyelin. PPMP (10 μM), like C6-ceramide, caused an inhibition of the L-channel current as a function of time (Fig. 6A). The onset of inhibition caused by PPMP occurred within 4–6 min after drug addition, and maximal inhibition was observed between 14–16 min. The inhibition of the L-channel current persisted in BayK 8644-treated cells (Fig. 6B).

Sphingomyelinase (0.1 U/ml), like PPMP, inhibited the L-channel current (Fig. 6, A and B). The onset of inhibition caused by sphingomyelinase occurred within 6–8 min after drug addition, and a 30% reduction was observed after 17 min. These results indicate that preventing the breakdown of ceramide or increasing membrane hydrolysis of sphingomyelin causes an inhibitory effect on the L-channel current similar to that seen after the addition of C6-ceramide.

Lavendustin A, but not H7, attenuates the effect of ceramide on the L-channel current

Ceramides have been shown to stimulate different enzymes, including a ceramide-activated proline-directed protein kinase, Jun N-terminal kinase, Raf-K, and tyrosine kinase (26–28). Therefore, it is possible that the effect of ceramide can be attenuated by a kinase inhibitor. This was examined by pretreating the cells with different serine/threonine kinase inhibitors or lavendustin A, a tyrosine kinase inhibitor (29). Treatment with H7 (100 μM) alone, a nonspecific serine/threonine kinase inhibitor, for 10 min caused a small inhibition of the L-channel current (Fig. 7A). Pretreatment with H7 for 10 min had no effect on the inhibitory action of C6-ceramide (30 μM) on the L-channel current (Fig. 7A).

The effects of two selective protein kinase inhibitors were also determined. Pretreatment with KT5823 (1 μM), a selective protein kinase G inhibitor, for 10 min did not affect the inhibition by C6-ceramide (71.5 ± 3.4% *vs.* 72.1 ± 5.1% of control current in the presence or absence of KT5823; n = 4). A selective protein kinase A inhibitor, H89 (0.5 μM), also had no effect on the inhibition by C6-ceramide (data not shown). In contrast, treatment with lavendustin A (3 μM) alone reduced the L-channel current by 11.5% (Fig. 7B). The inhibitory effect of C6-ceramide was attenuated (from 26.7% to 16.9%) in lavendustin A-pretreated cells (Fig. 7B). The attenuation was not observed in cells pretreated with lavendustin B (3 μM), the inactive analog of lavendustin A (data not shown).

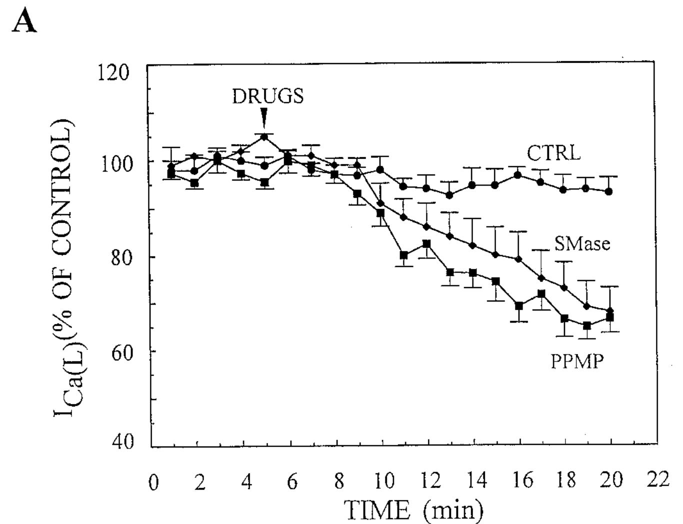

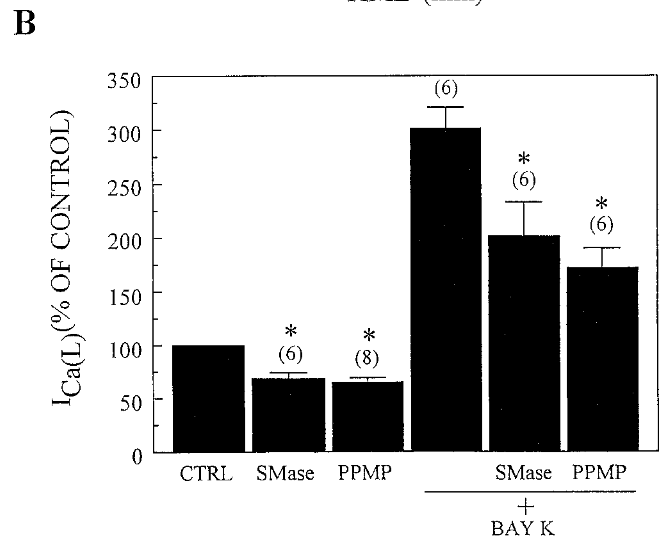

FIG. 6. Effect of PPMP and sphingomyelinase on the L-channel current in rat pinealocytes as a function of time. A, The effect of PPMP (a glucosylceramide synthase inhibitor; 10 μM) and sphingomyelinase (SMase; 0.1 U/ml) on L-channel current as a function of time. The data were analyzed as described in Fig. 4. Shown for comparison is the L-channel current run down (CTRL). Both SMase and PPMP were effective in decreasing the L-channel current. The time course of the inhibition was similar to that produced by C2- and C6-ceramide. B, The data obtained 15 min after the addition of PPMP and SMase. Also shown in B is the decrease in L-channel current caused by PPMP and SMase in cells pretreated with BayK 8644 (1 μM) for 5 min. The n values are shown in *parentheses above the bars*. *, $P < 0.05$ compared with the corresponding control current.

Interleukin-1β inhibits the L-channel current

Several cytokines, including interleukin-1β, tumor necrosis factor-α, and interferon-γ, are known to induce sphingomyelin hydrolysis to ceramide (8, 9). As abundant expression of interleukin-1β and its specific receptor has been demonstrated in the rat pineal gland (30), the effect of interleukin-1β on the L-channel current was examined. Interleukin-1β (10 ng/ml), like C6-ceramide, also inhibited the L-channel current (Fig. 8A). The onset of inhibition caused by interleukin-1β occurred within 8–10 min, and the maximal inhibition was observed between 14–16 min (Fig. 8B). Heat-inactivated

Downloaded from https://academic.oup.com/endo/article/140/12/5682/2990682 by guest on 20 August 2022

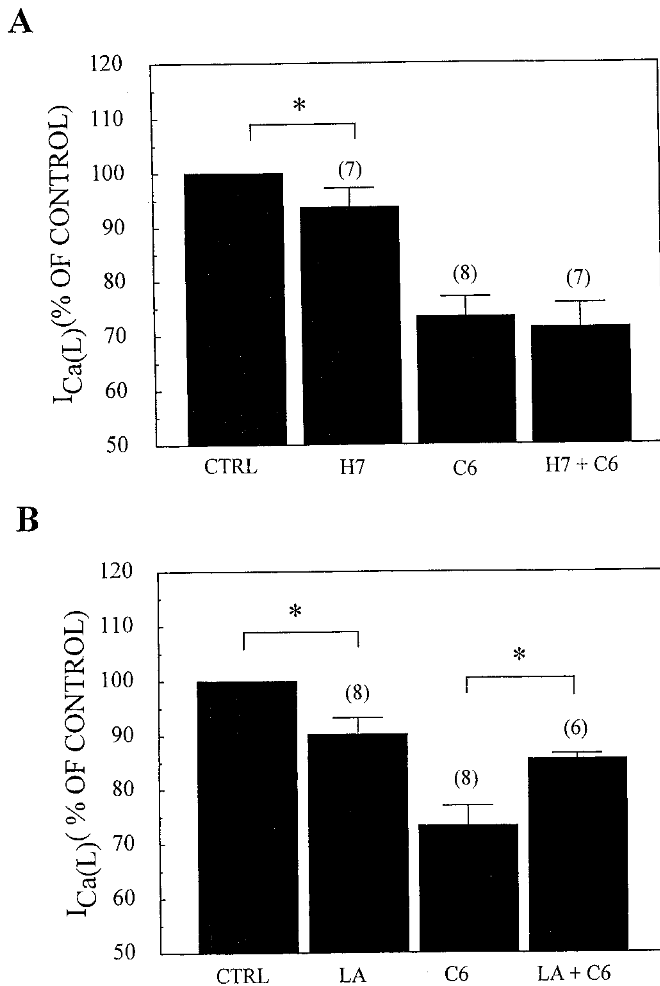

FIG. 7. Effect of H7 and lavendustin A on the C6-ceramide-mediated inhibition of L-channel currents in rat pinealocytes. A, H7 (100 μM; n = 7) caused a small inhibition of the L-channel current. In cells pretreated with H7 (100 μM; n = 7) for 10 min, C6-ceramide (C6; 30 μM) was effective in reducing the L-channel current. Shown for comparison is the effect of C6 (30 μM; n = 8; see *Materials and Methods*). B, Lavendustin A (LA; 3 μM; n = 8) caused a small decrease in the L-channel current. In cells pretreated with LA (3 μM; n = 6) for 10 min, the inhibition caused by C6 was attenuated. Shown for comparison is the effect of C6 (30 μM; n = 8). The n values are shown in *parentheses above the bars*. *, $P < 0.05$, compared with treatment without the kinase inhibitor.

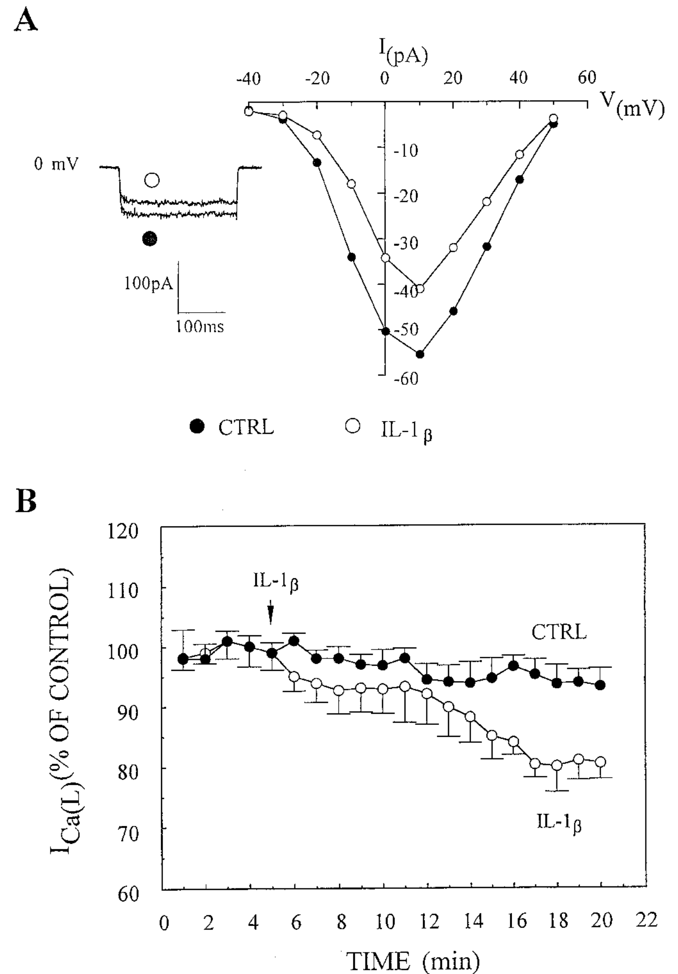

FIG. 8. Effect of interleukin-1β on the L-channel current in rat pinealocytes. A, The L-channel current is activated by depolarizing a pinealocyte from −50 to 0 mV in the absence or presence of interleukin-1β (IL-1β; 10 ng/ml). The I-V relationships obtained from the same cell are shown on the *right*. IL-1β was effective in decreasing the L-channel current. B, The effect of IL-1β (10 ng/ml) on the L-channel current as a function of time. The data were analyzed as described in Fig. 4.

interleukin-1β had no effect on the L-channel current (data not shown).

Discussion

Signaling through the sphingomyelin pathway, which is present in most mammalian cells, has generally been accepted as an important mechanism in regulating cellular processes such as growth, differentiation, apoptosis, and cell cycle arrest (31, 32). Activation of this pathway involves generation of ceramide through hydrolysis of sphingomyelin by sphingomyelinase. The ceramide produced, which acts a second messenger, has been shown to modulate the activities of different kinases as well as phosphatases in mediating its biological responses (10–13). However, results from the present study suggest that ceramide, probably through activation of tyrosine kinases, also acts as an important modulator of the L-channel current.

Our earlier study on the effect of ceramide indicated that it inhibited the potentiation of cAMP and cGMP accumulation caused by $[Ca^{2+}]_i$-elevating agents but not that caused by an activator of protein kinase C or an α_1-adrenergic agonist (16). Among the different $[Ca^{2+}]_i$-elevating agents, C6-ceramide was only effective in inhibiting the potentiation caused by a depolarizing concentration of K^+ or by BayK 8644, agents that act specifically on the voltage-gated Ca^{2+} channels. C6-ceramide did not inhibit the potentiation caused by phenylephrine, ionomycin, or thapsigargin, three agents that elevate $[Ca^{2+}]_i$ through different mechanisms. In this study, it was found that C6-ceramide caused an increase in the EC_{50} of the potentiation caused by depolarizing concentrations of K^+, suggesting that ceramide may affect the responsiveness of the L-channels to depolarization.

Downloaded from https://academic.oup.com/endo/article/140/12/5682/2990682 by guest on 20 August 2022

By measuring $[Ca^{2+}]_i$ directly, we were able to show that only $[Ca^{2+}]_i$ changes mediated through the voltage-gated Ca^{2+} channels are affected by ceramide. In contrast, ceramide has no effect on the norepinephrine-mediated increase in $[Ca^{2+}]_i$, which is independent of the L-channel (33) but dependent on release from intracellular stores (34) and influx through a receptor-mediated mechanism (33). Together these data provide indirect evidence that in its inhibition of the potentiation of the cyclic nucleotide responses, ceramide is selectively preventing the elevation of $[Ca^{2+}]_i$ via the L-type Ca^{2+} channel rather than inhibiting a Ca^{2+}-mediated event.

Using the whole cell version of the patch-clamp technique, we have confirmed that ceramide has an inhibitory effect on the L-type Ca^{2+} channel current. This is the first report of an effect of ceramide on the α_{1D}-subtype of Ca^{2+} channels (4) that are commonly found in neuroendocrine cells (35). Although ceramide caused a decrease in the peak L-channel current, there was no detectable shift in the potential at which the peak inward current occurred after treatment with C6-ceramide. However, studies with deactivation tail currents showed that C6-ceramide shifted the activation toward more positive potentials, suggesting that C6-ceramide may modify gating of these channels.

Even though our results with ceramide are obtained with C2- and C6-ceramide, two synthetic structural analogs of the naturally occurring ceramide, additional data suggest that generating ceramide endogenously has a similar effect on the L-type Ca^{2+} channel. This is based on the observations that treatment with PPMP, which inhibits the metabolism of ceramide and elevates cellular ceramide level (24, 25) is effective in inhibiting the L-channel current. Furthermore, treatment with exogenous sphingomyelinase, which induces the hydrolysis of sphingomyelin, also has the same effect as C2- or C6-ceramide. These results suggest that C2- and C6-ceramide, the synthetic ceramides, are simulating the effects of endogenously produced ceramide, a second messenger generated in the sphingomyelin cycle.

With regard to the mechanism through which ceramide inhibits the L-type Ca^{2+} channel current, ceramide has been shown to activate a novel serine/threonine protein kinase (27). However, our result argues against the involvement of this kinase in the effect of ceramide on the L-channel current, as pretreatment with a serine/threonine kinase inhibitor, H7, has no effect on the inhibition by ceramide. Although we have previously shown that the effect of ceramide on cyclic nucleotide accumulation is mediated through phosphodiesterases (16), this mechanism cannot explain its effect on the L-channel current. This is based on the observations that neither H89, a selective protein kinase A inhibitor, nor KT5823, a selective protein kinase G inhibitor, influences the effect of ceramide. Another downstream effect of ceramide is the stimulation of a cytosolic protein phosphatase (10). Although the L-channel current in rat pinealocytes can be regulated by protein phosphatases, inhibition of protein phosphatase activities reduces rather than enhances the L-channel current (15). Therefore, it is unlikely that activation of protein phosphatase is mediating the inhibitory effect of ceramide on the channel.

Another possible mechanism is that increasing the level of ceramide in the lipid bilayer may have a nonspecific lipid effect on the channels. However, this is unlikely, because both C2- and C6-ceramide produce similar effects on the current, but C2-dihydroceramide, an inactive analog of ceramide, is without effect. Furthermore, the effect of C6-ceramide can be blocked by a tyrosine kinase inhibitor. Indeed, the attenuation of the effect of ceramide by lavendustin A, a tyrosine kinase inhibitor, points toward a signaling cascade from ceramide via tyrosine kinase to the L-channel. It is of interest that the effect of ceramide on the channels in T lymphocytes is also mediated by tyrosine kinases (36). Although the identity of the specific tyrosine kinase involved remains unclear, our result suggests that ceramide is using a specific signaling pathway in mediating its effect on the L-channel. As treatment with lavendustin A also causes a small reduction of the L-channel current, tyrosine kinase appears to have a tonic effect on the basal activity of the L-channel current.

Extracellular messengers that are capable of signaling through the sphingomyelin cycle in different cell types include tumor necrosis factor-α, interleukin-1β, interferon-γ, and nerve growth factor (7–9). Among these messengers, there is a high expression of interleukin-1β and its receptors in the rat pineal gland (30). In this study, treatment with interleukin-1β was found to have an inhibitory effect on the L-channel current in this tissue, suggesting that interleukin-1β may be an activator of the sphingomyelin pathway in the rat pineal gland. Although nerve growth factor is also present in the pineal gland, it has no effect on the L-channel current (5).

The pineal gland predominantly expresses the α_{1D}-subtype of Ca^{2+} channels (4). This channel is commonly found in neuronal and neuroendocrine cells (35). The modulation of L-channels by ceramide represents another signaling mechanism through which these channels can be regulated in the rat pineal gland and probably other neuronal tissue. Within the pinealocytes, this regulation may be of physiological importance, as these channels are involved in the control of pineal function, including melatonin synthesis (2). It has recently been shown that acetylcholine, which depolarizes these channels, has an inhibitory effect on melatonin synthesis through the vesicular release of glutamate (2). However, it remains to be determined whether the sphingomyelin cycle has a role to play in melatonin synthesis. Nonetheless, $[Ca^{2+}]_i$ has been shown to modulate the adrenergically mediated induction of *N*-acetyltransferase, the rate-limiting enzyme in melatonin production (37).

The observed effect of ceramide on the L-channels may have a more general implication apart from its contribution to pineal physiology. Our observations suggest that the sphingomyelin pathway may play an important role in the regulation of any cellular events that involve the L-channels. Considering the widespread distribution of L-channels and the physiological processes regulated by these channels (38), the potential exits that the sphingomyelin cycle may regulate cellular processes other than the established ceramide-mediated physiological events (32). In this regard, ceramide also regulates the L-channels in rat ventricular myocytes (6). Indeed, the ceramide effect on L-channels may represent one of the downstream mechanisms through which ceramide

Downloaded from https://academic.oup.com/endo/article/140/12/5682/2990682 by guest on 20 August 2022

mediates its established effects on apoptosis, cell growth, and differentiation (32).

In summary, based on $[Ca^{2+}]_i$ measurement and patch-clamp studies, our results support an inhibitory effect of ceramide on the α_{1D}-subtype of Ca^{2+} channels, the specific subtype of L-channels expressed in rat pinealocytes (4). Furthermore, tyrosine kinase appears to be involved in this effect of ceramide. Although interleukin-1β can inhibit this channel, it remains to be determined whether this cytokine can activate the sphingomyelin cycle in the rat pineal gland. Our results are of importance not only to the understanding of pineal physiology, but also to neuroendocrinology in general.

Acknowledgment

The authors thank Dr. Albert Baukal (NICHHD, NIH) for the supply of antisera for the RIA.

References

1. **Letz B, Schomerus C, Maronde E, Korf HW, Horbmacher C** 1997 Stimulation of a nicotinic ACh receptor causes depolarization and activation of L-type Ca^{2+} channels in rat pinealocytes. J Physiol 499:329–340
2. **Yamada H, Ogura A, Koizumi S, Yamaguchi A, Moriyama Y** 1998 Acetylcholine triggers L-glutamate exocytosis via nicotinic receptors and inhibits melatonin synthesis in rat pinealocytes. J Neurosci 18:4946–4952
3. **Chik CL, Liu Q-Y, Li B, Karpinski E, Ho AK** 1995 cGMP inhibits L-type Ca^{2+} channel currents through protein phosphorylation in rat pinealocytes. J Neurosci 15:3104–3109
4. **Chik CL, Liu Q-Y, Li B, Klein DC, Zylka M, Kim DS, Chin H, Karpinski E, Ho AK** 1997 α_{1D} L-type Ca^{2+} channel currents: inhibition by a β-adrenergic agonist and pituitary adenylate cyclase-activating polypeptide (PACAP) in rat pinealocytes. J Neurochem 68:1078–1087
5. **Chik CL, Li B, Karpinski E, Ho AK** 1997 Insulin and insulin-like growth factor-1 inhibit the L-type Ca^{2+} channel current in rat pinealocytes. Endocrinology 138:2033–2042
6. **Schreur KD, Liu S** 1997 Involvement of ceramide in inhibitory effect of IL-1β on L-type Ca^{2+} current in adult rat ventricular myocytes. Am J Physiol 272:H2591–H2598
7. **Kim M-Y, Linardic C, Obeid L, Hannun Y** 1991 Identification of sphingomyelin turnover as an effector mechanism for the action of tumor necrosis factor α and γ-interferon. J Biol Chem 266:484–489
8. **Hannun YA** 1994 The sphingomyelin cycle and the second messenger function of ceramide. J Biol Chem 267:3125–3128
9. **Kolesnick R, Golde DW** 1994 The sphingomyelin pathway in tumor necrosis factor and interleukin-1 signaling. Cell 77:325–328
10. **Dobrowsky RT, Hannun YA** 1992 Ceramide stimulates a cytosolic protein phosphatase. J Biol Chem 267:5048–5051
11. **Younes A, Kahn DW, Besterman JM, Bittman R, Byun H-S, Kolesnick RN** 1992 Ceramide is a competitive inhibitor of diacylglycerol kinase *in vitro* and in intact human leukemia (HL-60) cells. J Biol Chem 267:842–847
12. **Raines MA, Kolesnick RN, Golde DW** 1993 Sphingomyelinase and ceramide activate mitogen-activated protein kinase in myeloid HL-60 cells. J Biol Chem 268:14572–14575
13. **Lee JY, Hannun YA, Obeid LM** 1996 Ceramide inactivates cellular protein kinase Cα. J Biol Chem 271:13169–13174
14. **Abousalham A, Liossis C, O'Brien L, Brindley DN** 1997 Cell-permeable ceramides prevent the activation of phospholipase D by ADP-ribosylation factor and RhoA. J Biol Chem 272:1069–1075
15. **Chik CL, Li B, Karpinski E, Ho AK** 1999 Regulation of the L-type Ca^{2+} channel current in rat pinealocytes: role of basal phosphorylation. J Neurochem 72:73–80
16. **Negishi T, Chik CL, Ho AK** 1998 Ceramide selectively inhibits calcium-mediated potentiation of β-adrenergic-stimulated cyclic nucleotide accumulation in rat pinealocytes. Biochem Biophys Res Commun 244:57–61
17. **Buda M, Klein DC** 1978 A suspension culture of pinealocytes: regulation of *N*-acetyltransferase activity. Endocrinology 103:1483–1493
18. **Hamill OP, Marty A, Neher E, Sakmann B, Sigworth FJ** 1981 Improved patch-clamp techniques for high-resolution current recording from cells and cell-free membrane patches. Pflugers Arch 391:85–100
19. **Harper JF, Brooker G** 1975 Femtomole sensitive radioimmunoassay for cyclic AMP and cyclic GMP after 2′0 acetylation by acetic anhydride in aqueous solution. J Cyclic Nucleotide Res 1:207–218
20. **Ho AK, Chik CL, Klein DC** 1987 Protein kinase C is involved in adrenergic stimulation of pineal cGMP accumulation. J Biol Chem 262:10059–10064
21. **Ho AK, Ogiwara T, Chik CL** 1996 Thapsigargin modulates agonist-stimulated cAMP responses through cytosolic calcium-dependent and -independent mechanisms in rat pinealocytes. Mol Pharmacol 49:1104–1112
22. **Poenie M, Alderton J, Tsien RY, Steinhardt RA** 1985 Changes of free calcium levels with stages of the cell division cycle. Nature 315:147–149
23. **Chik CL, Ho AK** 1989 Multiple receptor regulation of cyclic nucleotides in rat pinealocytes. Prog Biophys Mol Biol 53:197–203
24. **Inokuchi J, Radin NS** 1987 Preparation of the active isomer of 1-phenyl-2-decanoylamino-3-morpholino-1-propanol, inhibitor of murine glucocerebroside synthetase. J Lipid Res 28:565–571
25. **de Chaves EIP, Bussiere M, Vance DE, Campenot RB, Vance JE** 1997 Elevation of ceramide within distal neurites inhibits neurite growth in cultured rat sympathetic neurons. J Biol Chem 272:3028–3035
26. **Cifone MG, Roncaioli P, de Maria R, Camarda G, Santoni A, Ruberti G, Testi R** 1995 Multiple pathways originate at the Fas/APO-1 (CD95) receptor: sequential involvement of phosphatidylcholine-specific phospholipase C and acidic sphingomyelinase in the propagation of the apoptotic signal. EMBO J 14:5859–5868
27. **Tian Q, Taupin J, Elledge S, Robertson M, Anderson P** 1995 Fas-activated serine/threonine kinase (FAST) phosphorylates TIA-1 during Fas-mediated apoptosis. J Exp Med 182:865–874
28. **Latinis KM, Koretzky GA** 1996 Fas ligation induces apoptosis and Jun kinase activation independently of CD45 and Lck in human T cells. Blood 87:871–875
29. **Hsu C-Y, Persons PE, Spada AP, Bednar RA, Levitzki A, Zilberstein A** 1991 Kinetic analysis of the inhibition of the epidermal growth factor receptor tyrosine kinase by lavendustin A and its analogue. J Biol Chem 266:21105–21112
30. **Wong M-L, Bongiorno PB, Rettori V, McCann SM, Licinio J** 1997 Interleukin (IL) 1β, IL-1 receptor antagonist, IL-10, and IL-13 gene expression in the central nervous system and anterior pituitary during systemic inflammation: pathophysiological implications. Proc Natl Acad Sci USA 94:227–232
31. **Hannun YA, Bell RM** 1989 Functions of phospholipids and sphingolipid breakdown products in cellular regulation. Science 243:500–507
32. **Perry DK, Hannun YA** 1998 The role of ceramide in cell signaling. Biochim Biophys Acta 1436:233–243
33. **Sugden LA, Sugden D, Klein DC** 1987 α1-Adrenoceptor activation elevates cytosolic calcium in rat pinealocytes by increasing net influx. J Biol Chem 262:741–745
34. **Saez JC, Moreno AP, Spray DC** 1994 Norepinephrine induces Ca^{2+} release from intracellular stores in rat pinealocytes. J Pineal Res 16:57–64
35. **Hofmann F, Biel M, Flockerzi V** 1994 Molecular basis for Ca^{2+} channel diversity. Annu Rev Neurosci 17:399–418
36. **Gulbins E, Szabo I, Baltzer K, Lang F** 1997 Ceramide-induced inhibition of T lymphocyte voltage-gated potassium channel is mediated by tyrosine kinases. Proc Natl Acad Sci USA 94:7661–7666
37. **Yu L, Schaad NC, Klein DC** 1993 Calcium potentiates cyclic AMP stimulation of pineal arylalkylamine *N*-acetyltransferase. J Neurochem 60:1436–1443
38. **Tsien RW, Ellinor PT, Horne WA** 1991 Molecular diversity of voltage-dependent Ca^{2+} channels. Trends Pharmacol Sci 12:349–354

Downloaded from https://academic.oup.com/endo/article/140/12/5682/2990682 by guest on 20 August 2022